

Transmit Antenna Selection in Vehicle-to-Vehicle Time-Varying Fading Channels

Petros S. Bithas¹, Athanasios G. Kanatas¹, Daniel B. da Costa², and Prabhat Kumar Upadhyay³

¹Department of Digital Systems, University of Piraeus, Greece

²Department of Computer Engineering, Federal University of Ceará (UFC), Sobral, CE, Brazil

³ Discipline of Electrical Engineering, Indian Institute of Technology Indore, Madhya Pradesh, India
e-mail: {pbithas;kanatas}@unipi.gr, danielbcosta@ieee.org, pkupadhyay@iiti.ac.in

Abstract—Transmit antenna selection (TAS) schemes have been adopted in various communication systems to provide improved performance with relatively reduced complexity. The quality-of-service (QoS) in these systems depends on the availability of perfect channel state information (CSI). In practice, it is difficult to acquire perfect CSI, since it may get outdated due to feedback process. In this paper, we investigate the impact of outdated CSI in a TAS system that operates in a vehicle-to-vehicle (V2V) communication environment. The V2V channel is modeled by the double-Weibull (DW) distribution, a widely adopted distribution for modelling scenarios where both the transmitter and the receiver are in motion. In this context, we introduce and derive important statistical metrics for the bivariate DW distribution, such as the probability density function, the cumulative distribution function, and the moments. Based on them, exact expressions for the outage probability and the average bit error probability of the TAS scheme are derived under the assumption of outdated CSI. Moreover, simplified asymptotic closed-form expressions have been obtained. These expressions are then used to study the performance of the system under consideration.

Index Terms—Correlated double-Weibull fading, outdated channel estimations, quality-of-service, transmit antenna selection, vehicle-to-vehicle communications.

I. INTRODUCTION

Intervehicular communication (IVC) systems have gained an increased interest by the academic community and the industry over the past several years. These systems enable the vehicle-to-vehicle (V2V) and vehicle-to-infrastructure communications and can be used in a variety of application scenarios, including road-safety, energy-saving improvements, infotainment. However, in contrast to the traditional cellular-mobile radio link, the V2V propagation channel is much more dynamic, since it consists of two mobile transceivers that are both closely located to the ground level. As far as the V2V channel fading statistics are concerned, several models have been proposed, which are mainly based on the double-scattering radio propagation channel [1]. The basic principle in this model is that the envelope of the resulting impulse response is actually a multiplication of two independent envelopes, due to the double-bouncing mechanism. In this context, several approaches have been proposed including double-Rayleigh [2], double-Nakagami [3], and double-Weibull (DW) [4]. Using these new families of distributions, the performance of various communication systems has been evaluated in IVC

scenarios, e.g., diversity systems [5], cooperative communications [6], [7], automatic repeat request [8].

An important aspect that should also be taken into consideration in IVC systems is the size and power limitations that exist due to the constraints that are imposed by the vehicle. A well-known technique that is found to clearly improve the system's performance without considerably increasing the overall complexity is the transmit antenna selection (TAS). In this scheme, a single transmit antenna that maximizes the total received signal power at the receiver (Rx) is selected for transmission [9]. This "simple" and effective approach has gained the interest of many researchers and consequently has been adopted in various communication scenarios, including cooperative communications [10] and security enhancement techniques [11]. Despite the benefits that TAS scheme offers to the system's quality-of-service (QoS), its performance depends on the availability of perfect channel state information (CSI). However, in practical cases due to channel estimation errors and/or feedback delays, such an ideal assumption has only theoretical importance and cannot be established, especially in mobile networks [12]. Owing to this fact, the performance of TAS systems under the assumption of outdated CSI has been investigated in various (cellular-based) communication scenarios [13]–[15]. Nevertheless, to the best of the authors' knowledge, the performance of TAS in DW modeled V2V communication scenarios has not been investigated in the literature yet and thus motivates this work.

In this paper, an analytical study of the impact of outdated CSI on the performance of a V2V communication system that supports TAS is performed. The analysis is based on a well-established channel model for mobile-to-mobile communications, which is the DW. In order to investigate the effects of outdated CSI in this scenario, the bivariate DW distribution is introduced and studied. In particular, important statistical characteristics of the bivariate DW distribution, namely the probability density function (PDF), cumulative distribution function (CDF), and the moments, are presented for the first time. The new expressions are used to model the correlation between the exact and outdated versions of the received signal-to-noise ratio (SNR) in a V2V TAS communication scenario. Under this context, the QoS is evaluated using the criteria of outage probability (OP) and average bit error probability (ABEP).

The results are obtained in exact analytical expressions that allow fast and efficient evaluations of the performance, thereby avoiding the time consuming simulations.

The rest of the paper is organized as follows. In Section II, the bivariate statistics of the DW distribution are presented. In Section III, the system and channel models of the TAS scheme are presented along with a stochastic analysis for the received SNR statistics. In Section IV, this analysis is used to study the OP and the ABEP performance measures. In Section V, several numerical performance results are presented and discussed, while in Section VI, the concluding remarks are provided.

II. BIVARIATE STATISTICS

Let $X_j, X_{j+1}, j \in \{1, 3\}$, be two correlated Weibull random variables (RVs) with joint PDF given by [16, eq. (11)]

$$f_{X_j, X_{j+1}}(x_1, x_2) = \frac{\beta_1 \beta_2 x_1^{\beta_1 - 1} x_2^{\beta_2 - 1}}{\Omega_j \Omega_{j+1} (1 - \rho_i)} \exp \left[-\frac{1}{(1 - \rho_i)} \right] \times \left(\frac{x_1^{\beta_1}}{\Omega_j} + \frac{x_2^{\beta_2}}{\Omega_{j+1}} \right) I_0 \left[\frac{2x_1^{\beta_1/2} x_2^{\beta_2/2} \rho_i}{\sqrt{\Omega_j \Omega_{j+1}} (1 - \rho_i)} \right] \quad (1)$$

where $\Omega_j = [\mathbb{E} \langle X_j^2 \rangle / \Gamma(1 + 2/\beta_1)]^{\beta_1/2}$, $\Omega_{j+1} = [\mathbb{E} \langle X_{j+1}^2 \rangle / \Gamma(1 + 2/\beta_2)]^{\beta_2/2}$, with $\mathbb{E} \langle \cdot \rangle$ denoting expectation, $\Gamma(\cdot)$ is the Gamma function [17, eq. (8.310/1)], $I_v(\cdot)$ is the modified Bessel function of the first kind and order v [17, eq. (8.445)], and β_1, β_2 denote the Weibull shaping parameters. Moreover, in (1), $0 \leq \rho_i < 1$, with $i \in \{1, 2\}$, is the power correlation coefficient defined as

$$\rho_i \triangleq \frac{\text{cov}(X_j^2, X_{j+1}^2)}{\sqrt{\text{var}(X_j^2) \text{var}(X_{j+1}^2)}} \quad (2)$$

where $\text{cov}(\cdot)$ and $\text{var}(\cdot)$ stand for the covariance and variance, respectively. Let Z_1, Z_2 denote two DW RVs which are defined as the product of two independent Weibull RVs, i.e.,

$$\begin{array}{ccc} Z_1 = X_1 \times X_3 & & \\ \rho_{DW} \downarrow & \rho_1 \downarrow & \rho_2 \downarrow \\ Z_2 = X_2 \times X_4. & & \end{array} \quad (3)$$

In (3), ρ_i denotes the correlation coefficient between the Weibull RVs, defined in (2), and ρ_{DW} is the correlation coefficient of the corresponding DW RVs.

Applying the probability theory, the joint PDF of Z_1 and Z_2 is given by

$$f_{Z_1, Z_2}(z, w) = \int_0^\infty \int_0^\infty \frac{f_{X_1, X_2}(x, y)}{xy} f_{X_3, X_4} \left(\frac{z}{x}, \frac{w}{y} \right) dx dy. \quad (4)$$

Substituting (1) in (4), employing the infinite series representation of the Bessel function, [17, eq. (8.445)], making a change

of variables, and using [17, eq. (3.471/9)], an exact expression for the PDF of the bivariate DW distribution is extracted as

$$f_{Z_1, Z_2}(z, w) = \sum_{h, q=0}^{\infty} \frac{4\beta_1 \beta_2 \rho_1^q \rho_2^h}{(h!)^2 (q!)^2 \sqrt{\Omega_1 \Omega_2 \Omega_3 \Omega_4}} \times \frac{z^{\beta_1(1+\frac{p_1}{2})-1} w^{\beta_2(1+\frac{p_1}{2})-1}}{(\hat{\rho} \sqrt{\Omega_1 \Omega_2 \Omega_3 \Omega_4})^{p_1+1}} \times K_{p_2} \left(\frac{2z^{\beta_1/2}}{\sqrt{\hat{\rho} \Omega_1 \Omega_3}} \right) K_{p_2} \left(\frac{2w^{\beta_2/2}}{\sqrt{\hat{\rho} \Omega_2 \Omega_4}} \right) \quad (5)$$

where $\hat{\rho} = (1 - \rho_1)(1 - \rho_2)$, $p_1 = h + q$, $p_2 = h - q$, and $K_v(\cdot)$ is the modified Bessel function of the second kind and v th order [17, eq. (8.432/1)]. The joint CDF of Z_1 and Z_2 is given from $F_{Z_1, Z_2}(x, y) = \int_0^x \int_0^y f_{Z_1, Z_2}(z, w) dz dw$. Substituting (5) in this definition, representing Bessel function as in [18, eq. (14)], and then using [18, eq. (26)], the generic expression for the joint CDF of Z_1, Z_2 is deduced as

$$F_{Z_1, Z_2}(x, y) = \sum_{h, q=0}^{\infty} \frac{\rho_1^q \rho_2^h}{(h!)^2 (q!)^2 \sqrt{\Omega_1 \Omega_2 \Omega_3 \Omega_4}} \times \frac{x^{\beta_1(1+\frac{p_1}{2})} y^{\beta_2(1+\frac{p_1}{2})}}{(\hat{\rho} \sqrt{\Omega_1 \Omega_2 \Omega_3 \Omega_4})^{p_1+1}} \times \mathcal{G}_{1,3}^{2,1} \left(\frac{x^{\beta_1} / \hat{\rho}}{\Omega_1 \Omega_3} \middle| \frac{-\frac{p_1}{2}}{\frac{p_2}{2}, -\frac{p_2}{2}, -\frac{p_1}{2} - 1} \right) \mathcal{G}_{1,3}^{2,1} \left(\frac{y^{\beta_2} / \hat{\rho}}{\Omega_2 \Omega_4} \middle| \frac{-\frac{p_1}{2}}{\frac{p_2}{2}, -\frac{p_2}{2}, -\frac{p_1}{2} - 1} \right) \quad (6)$$

where $\mathcal{G}_{p,q}^{m,n}[\cdot]$ denotes the Meijer G-function [17, eq. (9.301)]. It is noted that the Meijer G-function is a built-in function in many mathematical software packages, e.g., Mathematica, Maple, and thus can be easily evaluated. Moreover, the rate of convergence of the infinite series given in (6) has been investigated. More specifically, the minimum number of terms, which guarantees accuracy better than $\pm 0.5\%$, is presented in Table I, for different values of $x = y, \Omega = \Omega_1 = \Omega_2 = \Omega_3 = \Omega_4, \beta = \beta_1 = \beta_2$, and $\rho = \rho_i$. From this table, it is clear that a relatively small number of terms is necessary to achieve an excellent accuracy. More specifically, this number of terms increases as x, y and/or ρ and/or β increase as well as with the decrease of Ω . It should be also noted that similar rate of convergence has been also observed for all the other infinite series expressions presented in this paper.

The joint moments of Z_1, Z_2 are defined as $\mu_{Z_1, Z_2}(n_1, n_2) \triangleq \mathbb{E} \langle Z_1^{n_1} Z_2^{n_2} \rangle$. Substituting (5) in this definition, making a change of variables, and using [17, eq. (6.561/16)], the joint moments of the bivariate DW distribution can be expressed as

$$\mu_{Z_1, Z_2}(n_1, n_2) = \hat{\rho}^{\frac{n_1}{\beta_1} + \frac{n_2}{\beta_2} + 1} (\Omega_1 \Omega_3)^{\frac{n_1}{\beta_1}} (\Omega_2 \Omega_4)^{\frac{n_2}{\beta_2}} \sum_{h, q=0}^{\infty} \frac{\rho_1^q \rho_2^h}{(h!)^2 (q!)^2} \prod_{i=1}^2 \Gamma \left(\frac{n_i}{\beta_i} + h + 1 \right) \Gamma \left(\frac{n_i}{\beta_i} + q + 1 \right). \quad (7)$$

Furthermore, using [17, eq. (9.100)] and after some mathematical manipulations, a closed-form expression for (7) can

TABLE I
MINIMUM NUMBER OF TERMS OF (6) REQUIRED FOR OBTAINING ACCURACY BETTER THAN $\pm 0.5\%$

		$\Omega = 10$		$\Omega = 20$	
		$\beta = 1.5$	$\beta = 2.5$	$\beta = 1.5$	$\beta = 2.5$
$\rho = 0.5$	x,y=1	2	2	2	2
	x,y=8	4	6	3	5
$\rho = 0.85$	x,y=1	10	10	7	7
	x,y=8	21	26	14	22

be derived as

$$\mu_{Z_1, Z_2}(n_1, n_2) = \hat{\rho}^{\frac{n_1}{\beta_1} + \frac{n_2}{\beta_2} + 1} (\Omega_1 \Omega_3)^{\frac{n_1}{\beta_1}} (\Omega_2 \Omega_4)^{\frac{n_2}{\beta_2}} \prod_{i=1}^2 \Gamma\left(\frac{n_i}{\beta_i} + 1\right)^2 {}_2F_1\left(\frac{n_1}{\beta_1} + 1, \frac{n_2}{\beta_2} + 1, 1, \rho_i\right) \quad (8)$$

with ${}_2F_1(\cdot)$ denoting the Gauss hypergeometric function [17, eq. (9.100)]. In order to determine the relation between the DW correlation coefficient, ρ_{DW} , and the corresponding Weibull ones, ρ_1, ρ_2 , the n th order moment of a single DW RV X_i is required and is given by

$$\mu_{X_i}(n_i) = (\Omega_i \Omega_{i+2})^{\frac{n_i}{\beta_i}} \Gamma\left(\frac{n_i}{\beta_i} + 1\right)^2. \quad (9)$$

Substituting (8) and (9) in the definition of the correlation coefficient given in (2) and after some simplifications, a simple closed-form expression for ρ_{DW} is obtained as

$$\rho_{DW} = \left\{ \prod_{i=1}^2 [(1 - \rho_i)]^{\frac{2}{\beta_1} + \frac{2}{\beta_2} + 1} {}_2F_1\left(\frac{2}{\beta_1} + 1, \frac{2}{\beta_2} + 1, 1, \rho_i\right) - 1 \right\} \prod_{i=1}^2 \frac{\Gamma\left(\frac{2}{\beta_i} + 1\right)^2}{\sqrt{\Gamma\left(\frac{4}{\beta_1} + 1\right)^2 - \Gamma\left(\frac{2}{\beta_i} + 1\right)^4}}. \quad (10)$$

In Fig. 1, based on (10), the correlation coefficient ρ_{DW} is plotted as a function of ρ_1, ρ_2 , which are considered to be equal. It is clear that ρ_{DW} also ranges between zero and one, while it is shown that as β_i increases, ρ_{DW} approaches ρ_1, ρ_2 .

III. TRANSMIT ANTENNA SELECTION IN TIME-VARYING FADING CHANNELS

We consider a communication system with 2 transmit antennas and one receive antenna that operates in an IVC environment modeled by the DW fading model. It is noted that the assumption of 2 transmit antennas is desirable in practical V2V systems, where major constraints exist in terms of space limitation, power consumption, and signal processing capabilities. In the system under consideration, the transmit antenna with the largest SNR is selected by the Rx. The transmitter (Tx) is informed for each decision based on an error-free feedback link. In this context, let $\gamma_i = |Z_i|^2 \frac{E_s}{N_0}$, with $i \in \{1, 2\}$, denoting the instantaneous SNR, with E_s being

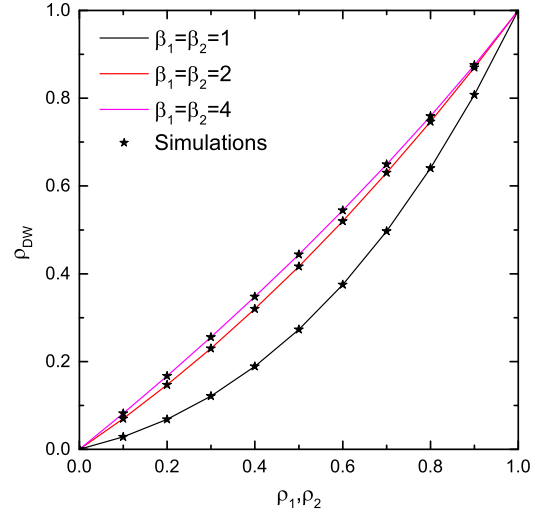


Fig. 1. The DW correlation coefficient ρ_{DW} as a function of ρ_1, ρ_2 .

the transmitted symbol energy and N_0 the noise variance. The marginal PDF of γ_i is given by [4]

$$f_{\gamma_i}(y) = \frac{\beta_i}{\bar{\gamma}_i^2} y^{\beta_i/2 - 1} K_0\left(2 \frac{y^{\beta_i/4}}{\bar{\gamma}_i}\right) \quad (11)$$

and the corresponding CDF is given by

$$F_{\gamma_i}(y) = 1 - \frac{2y^{\beta_i/4}}{\bar{\gamma}_i} K_1\left(2 \frac{y^{\beta_i/4}}{\bar{\gamma}_i}\right) \quad (12)$$

where $\bar{\gamma}_i = \Gamma(1 + 2/\beta_i) \Omega_i^{2/\beta_i} \frac{E_s}{N_0}$. Here, it is noted that as the value of β_i increases, the severity of fading decreases, while for $\beta_i = 2$, (11) reduces to the well-known double-Rayleigh PDF. In a V2V communication environment, it is very likely that the fading behavior will change rapidly due to the fast time varying nature of the medium. Hence, in this work, the CSI that is fed back to the Tx is assumed to be outdated, due to the delay naturally existing between the selection and data transmission phases. More specifically, the imperfection between the actual received SNR of the selected antenna at the data reception instance, γ_i , and $\tilde{\gamma}_i$, which is available during the selection phase, can be measured based on a correlation coefficient [14]. In that case, assuming i) the two links between the two antennas of the Tx and the corresponding one of the Rx are spatial uncorrelated and ii) characterized by different fading (shaping and scaling) parameters, the PDF of the actual

received SNR at the data reception instance, γ_{out} , can be expressed as

$$f_{\gamma_{\text{out}}}(x) = \sum_{i=1}^2 \int_0^{\infty} f_{\gamma_i, \bar{\gamma}_i}(y, x) F_{\gamma_{3-i}}(y) dy \quad (13)$$

where $F_{\gamma_{3-i}}(y)$ is given by (12). For evaluating (13), $f_{\gamma_i, \bar{\gamma}_i}(y, x)$ is required, which can be evaluated based on the results presented in the previous section. More specifically, assuming equal shaping and scaling parameters, for the time-correlated versions of each Tx-Rx link, and making a change of variables in (5), the expression for the joint PDF between γ_i and $\bar{\gamma}_i$ can be obtained as

$$f_{\gamma_i, \bar{\gamma}_i}(x, y) = \sum_{h,q=0}^{\infty} \frac{\beta_i^2 \rho_i^{p_1} / \bar{\gamma}_i^2}{(h!)^2 (q!)^2 ((1-\rho_i) \bar{\gamma}_i)^{2(p_1+1)}} \times (xy)^{\frac{\beta_i}{2} (\frac{p_1}{2} + 1) - 1} K_{p_2} \left[\frac{2x\beta_i^{1/4}}{\bar{\gamma}_i(1-\rho_i)} \right] K_{p_2} \left[\frac{2y\beta_i^{1/4}}{\bar{\gamma}_i(1-\rho_i)} \right]. \quad (14)$$

Therefore, based on (13) as well as (14), the CDF of γ_{out} is given by

$$F_{\gamma_{\text{out}}}(\gamma) = \sum_{i=1}^2 \sum_{h,q=0}^{\infty} \frac{\rho_i^{p_1} \gamma^{\frac{\beta_i}{2} (\frac{p_1}{2} + 1)} / \bar{\gamma}_i^2}{(h!)^2 (q!)^2 ((1-\rho_i) \bar{\gamma}_i)^{2(p_1+1)}} \times \mathcal{G}_{1,3}^{2,1} \left(\frac{\gamma^{\beta_i/2}}{((1-\rho_i) \bar{\gamma}_i)^2} \middle| \frac{-\frac{p_1}{2}}{\frac{p_2}{2}, -\frac{p_2}{2}, -\frac{p_1}{2} - 1} \right) \mathcal{S}_i \quad (15)$$

where

$$\mathcal{S}_i = \Gamma(h+1) \Gamma(q+1) - \frac{\beta_{3-i}^{p_1 + \frac{\beta_{3-i}}{\beta_i} + 1} ((1-\rho_i) \bar{\gamma}_i)^{\frac{\beta_{3-i}}{\beta_i}}}{\bar{\gamma}_{3-i} (2\pi)^3} \times \mathcal{G}_{2\beta_{3-i}, 2\beta_i}^{2\beta_i, 2\beta_{3-i}} \left(\frac{((1-\rho_i) \bar{\gamma}_i \beta_{3-i})^{2\beta_{3-i}}}{(\bar{\gamma}_{3-i} \beta_i)^{2\beta_i}} \right) \left| \frac{\Delta(\beta_{3-i}, -\frac{2h+\beta_{3-i}/\beta_i}{2}), \Delta(\beta_{3-i}, -\frac{2q+\beta_{3-i}/\beta_i}{2})}{\Delta(\beta_i, 1/2), \Delta(\beta_i, -1/2)} \right)$$

where $\Delta(k, a) = \frac{a}{k}, \frac{a+1}{k}, \dots, \frac{a+k-1}{k}$. The proof for (15) is given in the Appendix. Assuming the same fading conditions for both Tx-Rx links, (15) simplifies to

$$F_{\gamma_{\text{out}}}(\gamma) = 2 \sum_{h,q=0}^{\infty} \frac{\rho^{p_1} \gamma^{\frac{\beta}{2} (\frac{p_1}{2} + 1)} / \bar{\gamma}^2}{h! q! ((1-\rho) \bar{\gamma})^{p_1}} \times \mathcal{G}_{1,3}^{2,1} \left(\frac{\gamma^{\beta/2}}{((1-\rho) \bar{\gamma})^2} \middle| \frac{-\frac{p_1}{2}}{\frac{p_2}{2}, -\frac{p_2}{2}, -\frac{p_1}{2} - 1} \right) \left[1 - \frac{(1-\rho)^2}{\Gamma(p_1+3)} \times (h+1)!(q+1)! {}_2F_1 \left(h+2, q+2, p_1+3, 1 - (1-\rho)^2 \right) \right] \quad (16)$$

where $\rho = \rho_i$, $\beta = \beta_i$ and $\bar{\gamma} = \bar{\gamma}_i$.

IV. PERFORMANCE EVALUATION

In this section, using the previously derived expressions, analytical results for important metrics of the QoS, such as the OP and the ABER, are provided.

A. Outage Probability

The OP is defined as the probability that the instantaneous received SNR falls below a predetermined threshold γ_T . In this case, using (15) it can directly be evaluated as $P_{\text{out}} = F_{\gamma_{\text{out}}}(\gamma_T)$.

1) *Asymptotic Analysis*: In order to provide a simplified expression, the main concern is to derive an asymptotic closed-form expression for $F_{\gamma_{\text{out}}}(\gamma)$. Therefore, assuming $\rho = \rho_1 = \rho_2$, higher values of $\bar{\gamma}$, and using [19, eq. (03.02.06.0004.02)], the Bessel function in (1) can be approximated as $I_\nu(z) \approx \frac{1}{\Gamma(\nu+1)} \left(\frac{z}{2}\right)^\nu$. Using this approximated expression and the approach presented in Appendix, the closed-form asymptotic expression for the CDF of γ_{out} is obtained as

$$F_{\gamma_{\text{out}}}(\gamma) \approx (1-\rho)^2 [2 - (1-\rho)^2] \times {}_2F_1 [2, 2, 3, 1 - (1-\rho)^2] \left[1 - 2 \frac{\gamma^{\beta/4} K_1 \left(\frac{2\gamma^{\beta/4}}{(1-\rho)\bar{\gamma}} \right)}{(1-\rho)\bar{\gamma}} \right]. \quad (17)$$

B. Average Bit Error Probability

Using the CDF-based approach, the ABER is given by [20]

$$P_b = \int_0^{\infty} -P'_e(\gamma) F_{\gamma_{\text{out}}}(\gamma) d\gamma \quad (18)$$

where $-P'_e(\gamma)$ denotes the negative derivative of the conditional error probability. It is noted that for all the ABER expressions derived here, different fading parameters have been considered for the two Tx-Rx links.

1) *Differentially Binary Phase Shift Keying (DBPSK)*: For DBPSK modulation, $-P'_e(\gamma) = \alpha\beta \exp(-\beta\gamma)$, where $\alpha = 1/2, \beta = 1$ [20]. Substituting (15) in (18), employing [18, eq. (21)], and doing some mathematical manipulations yield

$$P_b = \sum_{i=1}^2 \sum_{h,q=0}^{\infty} \frac{\alpha \rho_i^{p_1} / \bar{\gamma}_i^2}{(h!)^2 (q!)^2 ((1-\rho_i) \bar{\gamma}_i)^{p_1}} \frac{(\beta_i/\beta)^{\frac{\beta_i}{2} (\frac{p_1}{2} + 1) + \frac{1}{2}}}{(2\pi)^{\frac{\beta_i+1}{2}} 2\beta^{1/2}} \times \mathcal{G}_{\beta_i+2,6}^{4,\beta_i+2} \left(\frac{(\beta_i/\beta)^{\beta_i}}{((1-\rho_i) 2\bar{\gamma}_i)^4} \middle| \frac{-\Delta(2, -\frac{p_1}{2}), \Delta(\beta_i, -\frac{\beta_i}{2} (\frac{p_1}{2} + 1))}{\Delta(2, \frac{p_2}{2}), -\Delta(2, \frac{p_2}{2}), \Delta(2, -\frac{p_1}{2} - 1)} \right) \mathcal{S}_i. \quad (19)$$

2) *Binary Phase Shift Keying (BPSK)*: For BPSK modulation, $-P'_e(\gamma) = \left(\frac{\alpha\sqrt{\beta}}{\sqrt{8\pi}}\right) \gamma^{-1/2} \exp(-\beta\gamma)$, where $\alpha = 1, \beta = 2$ [20]. Substituting (15) in (18), employing [18, eq. (21)], and doing some mathematical manipulations yield

$$P_b = \sum_{i=1}^2 \sum_{h,q=0}^{\infty} \frac{\rho_i^{p_1} \alpha \sqrt{2} / \bar{\gamma}_i^2}{(h!)^2 (q!)^2 ((1-\rho_i) \bar{\gamma}_i)^{p_1}} \frac{(2\beta_i/\beta)^{\frac{\beta_i}{4} (p_1+2)}}{4 (2\pi)^{\beta_i/2+1}} \times \mathcal{G}_{\beta_i+2,6}^{4,\beta_i+2} \left(\frac{(2\beta_i/\beta)^{\beta_i}}{(2(1-\rho_i) \bar{\gamma}_i)^4} \middle| \frac{-\Delta(2, -\frac{p_1}{2}), \Delta(\beta_i, \frac{1}{2} - \frac{\beta_i}{2} (\frac{p_1}{2} + 1))}{\Delta(2, \frac{p_2}{2}), -\Delta(2, \frac{p_2}{2}), \Delta(2, -\frac{p_1}{2} - 1)} \right) \mathcal{S}_i. \quad (20)$$

Since both ABER expressions derived in this section are based on (5), their convergence is fast due to the reduced number of terms that is employed, as shown in Table 1.

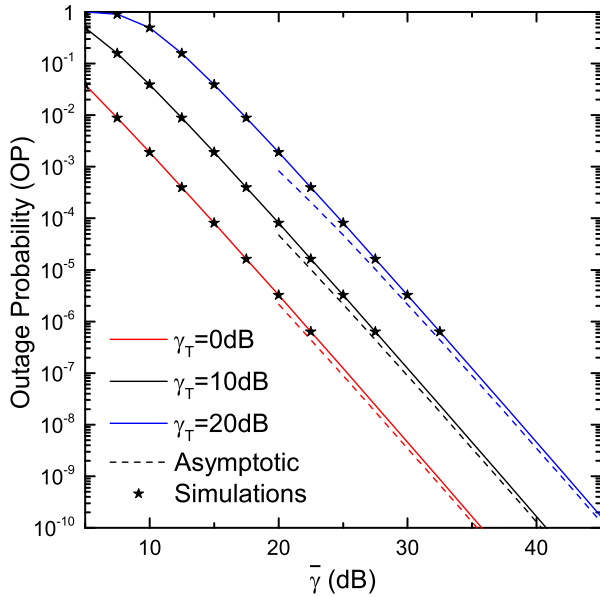


Fig. 2. OP vs $\bar{\gamma}$ for different values of γ_T .

V. NUMERICAL RESULTS

In this section, several numerically evaluated performance results are provided, using the criteria of OP and ABEP. It is noted that, for the simulated results, which are also included in the figures, correlated DW RVs have been generated using (3) and the approach presented in [16]. In Fig. 2, using (16) and (17), assuming equal fading parameters for the two Tx-Rx links and $\beta = 3, \rho = 0.75$, the OP is plotted as a function of the outage threshold γ_T . It is shown that the OP decreases with an increase on γ_T as well as on $\bar{\gamma}$. Moreover, the asymptotic curves, which are also included in the same figure, approximate quite well the exact ones, even for moderate values of the average SNR, that is for $\bar{\gamma} \geq 20$ dB. In Fig. 3, using (19), assuming different fading parameters for the two Tx-Rx links with $\beta_2 = \beta_1 + 1, \rho_1 = 0.8, \rho_2 = 0.85$, the ABEP of DBPSK is plotted as a function of the average SNR of the first antenna. In particular, the relationship between the average SNRs for the two Tx-Rx links is given by $\bar{\gamma}_i = \bar{\gamma}_1 \exp(-\delta(i-1))$, where δ is the power decaying factor, which has been set to $d = 0.5$, and $i \in [1, 2]$. In this figure, it is shown that the performance improves with an increase of the SNR as well as β_i . It is interesting to note that the performance improvement (due to the increase of β_i) decreases as β_i increases.

In Fig. 4, using (20) and assuming $\beta_1 = 2, \beta_2 = 3$, the ABEP of BPSK is plotted as a function of average received SNR of the first antenna for different values of ρ_i . In this figure, it is shown that as ρ_i increases, i.e., the SNR at the selection instance approaches the one at the reception instance, the performance improves. This performance improvement is higher for $\rho_i \rightarrow 1$. Finally, the simulation performance results, which are also included in all figures, verifying the validity of the proposed theoretical approach.

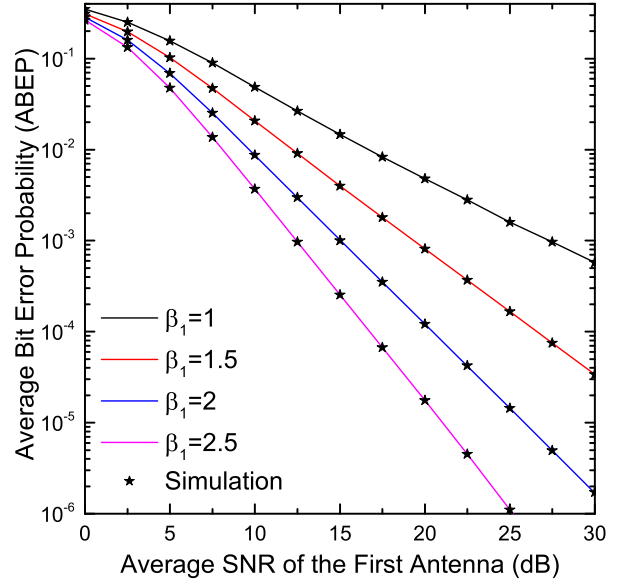


Fig. 3. ABEP vs $\bar{\gamma}_1$ for different values of the shaping parameters β_i .

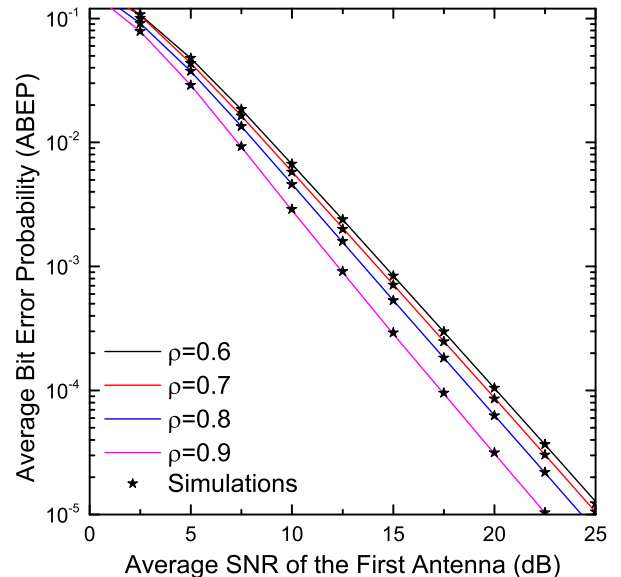


Fig. 4. ABEP vs $\bar{\gamma}_1$ for different values of the correlation coefficient ρ .

VI. CONCLUSIONS

The influence of outdated CSI on the performance of a TAS scheme operating in a V2V communication environment has been analytically investigated. For the purposes of the analysis, the bivariate DW distribution has been presented for the first time and used to model the correlation between the channel gains of the received signals at the selection and the data transmission instances. Considering non-identically distributed fading conditions, an analytical expression for the CDF of the output SNR was derived for the scheme under consideration. Based on this expression, the performance has been evaluated, using well-known metrics for the QoS, namely OP and ABEP.

It is depicted that outdated CSI affects seriously the system's performance, even when good channel conditions exist.

APPENDIX

In this Appendix, a proof for the derivation of (15) is presented. The CDF of the actual received SNR of the selected antenna is given by

$$F_{\gamma_{\text{out}}}(\gamma) = \sum_{i=1}^2 \int_0^{\gamma} \int_0^{\infty} f_{\gamma_i, \bar{\gamma}_i}(y, x) F_{\gamma_{3-i}}(y) dy dx. \quad (\text{A-1})$$

Substituting (14) and (12) in (A-1), the following three types of integrals appear

$$\begin{aligned} \mathcal{I}_1 &= \int_0^{\gamma} x^{\frac{\beta_i}{2}(\frac{p_1}{2}+1)-1} K_{p_2} \left(\frac{2x^{\beta_i/4}}{(1-\rho_i)\bar{\gamma}_i} \right) dx \\ \mathcal{I}_2 &= \int_0^{\infty} y^{\frac{\beta_i}{2}(\frac{p_1}{2}+1)-1} K_{p_2} \left(\frac{2y^{\beta_i/4}}{(1-\rho_i)\bar{\gamma}_i} \right) dy \\ \mathcal{I}_3 &= \int_0^{\infty} y^{\frac{\beta_i}{2}(\frac{p_1}{2}+1)+\frac{\beta_{3-i}}{4}-1} \\ &\quad \times K_{p_2} \left(\frac{2y^{\beta_i/4}}{(1-\rho_i)\bar{\gamma}_i} \right) K_1 \left(2\frac{y^{\beta_{3-i}/4}}{\bar{\gamma}_{3-i}} \right) dy. \end{aligned} \quad (\text{A-2})$$

For evaluating \mathcal{I}_1 , the Meijer G-function representation of the Bessel functions is employed, i.e., [18, eq. (14)]. Based on this representation, and with the aid of [18, eq. (26)], the solution of \mathcal{I}_1 is given as follows

$$\mathcal{I}_1 = \frac{\gamma^{\frac{\beta_i}{2}(\frac{p_1}{2}+1)}}{\beta_i} \mathcal{G}_{1,3}^{2,1} \left(\frac{\gamma^{\beta_i/2}}{((1-\rho_i)\bar{\gamma}_i)^2} \middle| \frac{-p_2}{\frac{p_2}{2}, -\frac{p_2}{2}, -\frac{p_2}{2}-1} \right). \quad (\text{A-3})$$

For evaluating \mathcal{I}_2 , [19, eq. (03.04.21.0116.01)] is employed, so that

$$\mathcal{I}_2 = \frac{((1-\rho_i)\bar{\gamma}_i)^{p_1+2}}{\beta_i} h! q!. \quad (\text{A-4})$$

For evaluating \mathcal{I}_3 , the Meijer G-function representation of the Bessel functions is also employed and with the aid of [18, eq. (21)], the solution of \mathcal{I}_3 is given as follows

$$\begin{aligned} \mathcal{I}_3 &= \frac{\beta_{3-i}^{p_1+\beta_2/\beta_1+1}}{2\beta_1} \frac{((1-\rho_i)\bar{\gamma}_i)^{p_1+\beta_2/\beta_1+2}}{(2\pi)^3} \\ &\quad \mathcal{G}_{2\beta_{3-i}, 2\beta_{3-i}}^{2\beta_i, 2\beta_{3-i}} \left(\frac{((1-\rho_i)\bar{\gamma}_i\beta_{3-i})^{2\beta_{3-i}}}{(\bar{\gamma}_{3-i}\beta_i)^{2\beta_i}} \right. \\ &\quad \left. \middle| \Delta(\beta_{3-i}, -\frac{2h+\beta_{3-i}/\beta_i}{2}), \Delta(\beta_{3-i}, -\frac{2q+\beta_{3-i}/\beta_i}{2}) \right). \end{aligned} \quad (\text{A-5})$$

Based on all these expressions and after some mathematical simplifications, (15) is finally derived.

ACKNOWLEDGEMENT

This research has received funding from the European Union's Horizon 2020 research and innovation programme under "ROADART" Grant Agreement No 636565.

REFERENCES

- [1] J. Salo, H. M. El-Sallabi, and P. Vainikainen, "Statistical analysis of the multiple scattering radio channel," *IEEE Trans. Antennas Propag.*, vol. 54, no. 11, pp. 3114–3124, Nov. 2006.
- [2] —, "Impact of double-Rayleigh fading on system performance," in *Proc. 1st IEEE Int. Symp. on Wireless Pervasive Computing, (ISWPC)*, 2006.
- [3] G. K. Karagiannidis, N. C. Sagias, and P. T. Mathiopoulos, "N*Nakagami: A novel stochastic model for cascaded fading channels," *IEEE Trans. Commun.*, vol. 55, no. 8, pp. 1453–1458, Aug. 2007.
- [4] N. C. Sagias and G. S. Tombras, "On the cascaded Weibull fading channel model," *Journal of the Franklin Institute*, vol. 344, no. 1, pp. 1–11, 2007.
- [5] A. Chelli, R. Hamdi, and M.-S. Alouini, "Channel modelling and performance analysis of V2I communication systems in blind bend scattering environments," *Progress In Electromagnetics Research B*, vol. 57, pp. 233–251, 2014.
- [6] H. Ilhan, M. Uysal, and I. Altunbas, "Cooperative diversity for intervehicular communication: Performance analysis and optimization," *IEEE Trans. Veh. Technol.*, vol. 58, no. 7, pp. 3301–3310, Sep. 2009.
- [7] P. S. Bithas, G. P. Efthymoglou, and A. G. Kanatas, "A cooperative relay selection scheme in v2v communications under interference and outdated esi," in *2016 IEEE 27th Annual International Symposium on Personal, Indoor, and Mobile Radio Communications (PIMRC)*, Sept 2016, pp. 1–6.
- [8] A. Chelli, E. Zedini, M. S. Alouini, J. R. Barry, and M. Pätzold, "Performance and delay analysis of hybrid ARQ with incremental redundancy over double Rayleigh fading channels," *IEEE Trans. Wireless Commun.*, vol. 13, no. 11, pp. 6245–6258, Nov. 2014.
- [9] Z. Chen, J. Yuan, and B. Vucetic, "Analysis of transmit antenna selection/maximal-ratio combining in Rayleigh fading channels," *IEEE Trans. Veh. Technol.*, vol. 54, no. 4, pp. 1312–1321, Jul. 2005.
- [10] S. W. Peters and R. W. Heath, "Nonregenerative MIMO relaying with optimal transmit antenna selection," *IEEE Signal Processing Letters*, vol. 15, pp. 421–424, 2008.
- [11] N. Yang, P. L. Yeoh, M. Elkashlan, R. Schober, and I. B. Collings, "Transmit antenna selection for security enhancement in MIMO wiretap channels," *IEEE Trans. Commun.*, vol. 61, no. 1, pp. 144–154, Jan. 2013.
- [12] X. Lei, W. Zhou, P. Fan, and L. Fan, "Impact of outdated channel state information on multiuser cooperative relay networks in co-channel interference environments," in *IEEE International Conference on Communications in China*, 2012, pp. 503–507.
- [13] G. Amarasinguriya, C. Tellambura, and M. Ardakani, "Joint relay and antenna selection for dual-hop amplify-and-forward MIMO relay networks," *IEEE Trans. Wireless Commun.*, vol. 11, no. 2, pp. 493–499, Feb. 2012.
- [14] N. S. Ferdinand, D. B. da Costa, and M. Latva-aho, "Effects of outdated CSI on the secrecy performance of MISO wiretap channels with transmit antenna selection," *IEEE Commun. Lett.*, vol. 17, no. 5, pp. 864–867, May 2013.
- [15] J. Guo, C. Pei, and H. Yang, "Performance analysis of TAS/MRC in MIMO relay systems with outdated CSI and co-channel interference," *IEEE Trans. Wireless Commun.*, vol. 13, no. 9, pp. 4848–4856, Sep. 2014.
- [16] N. C. Sagias and G. K. Karagiannidis, "Gaussian class multivariate Weibull distributions: theory and applications in fading channels," *IEEE Trans. Inf. Theory*, vol. 51, no. 10, pp. 3608–3619, Oct 2005.
- [17] I. S. Gradshteyn and I. M. Ryzhik, *Table of Integrals, Series, and Products*, 6th ed. New York: Academic Press, 2000.
- [18] V. S. Adamchik and O. I. Marichev, "The algorithm for calculating integrals of hypergeometric type functions and its realization in REDUCE system," in *International Conference on Symbolic and Algebraic Computation*, Tokyo, Japan, 1990, pp. 212–224.
- [19] The Wolfram Functions Site, 2016. [Online]. Available: <http://functions.wolfram.com>
- [20] Y. Chen and C. Tellambura, "Distribution functions of selection combiner output in equally correlated Rayleigh, Rician, and Nakagami-m fading channels," *IEEE Trans. Commun.*, vol. 52, no. 11, pp. 1948–1956, Nov 2004.